NATIONAL ADVISORY COMMITTEE FOR AERONAUTICS

TECHNICAL NOTE 2061

THE EFFECT OF RATE OF CHANGE OF ANGLE OF ATTACK ON THE MAXIMUM LIFT OF A SMALL MODEL

By Paul W. Harper and Roy E. Flanigan

Langley Aeronautical Laboratory
Langley Air Force Base, Va.

Washington
March 1950

NATIONAL ADVISORY COMMITTEE FOR AERONAUTICS

TECHNICAL NOTE 2061

THE EFFECT OF RATE OF CHANGE OF ANGLE OF ATTACK ON THE MAXIMUM LIFT OF A SMALL MODEL

By Paul W. Harper and Roy E. Flanigan

SUMMARY

A wind-tunnel investigation was conducted of a $\frac{1}{20}$-scale partial model of a conventional fighter airplane to determine the effects of rate of change of angle of attack on its maximum lift. The tests were intended to supplement previous tests of the same model by extending the range of variables. The present tests covered a Mach number range from approximately 0.10 to 0.80 at pitching velocities varying from nearly 0 to about 20 radians per second.

The results showed that the maximum lift coefficient increased linearly with pitching velocity up to a limit value of the lift coefficient which depended on the Mach number. The magnitude of the pitching-velocity effect on the maximum lift coefficient decreased with increasing Mach number so that it became negligible for a Mach number of about 0.60.

INTRODUCTION

The rate of change of angle of attack has in recent years assumed appreciable significance among the parameters affecting the maximum wing loads and therefore the maneuverability of high-speed aircraft and missiles. Since the dynamic nature of this parameter has precluded investigations of its effect by the usual wind-tunnel-test procedures, a technique has been employed whereby a model was made to rotate in a manner simulating the motion of an airplane during pull-ups of varying abruptness. Results of a wind-tunnel investigation using this technique on a $\frac{1}{20}$-scale model of a conventional fighter airplane were presented in reference 1 for a Mach number range from about 0.20 to 0.60 with pitching velocities varying from about 3 to 12 radians per second and compared with flight results for the same airplane.

The satisfactory agreement obtained in the comparison indicated that model results could be used to predict maximum lift for full-scale flight conditions and, therefore, prompted further tests on the same

model over extended ranges of pitching velocity and Mach number primarily to determine a limiting value of the maximum lift coefficient, the extent of the maximum-lift-coefficient increment above the value for steady conditions, and the Mach number range in which pitching velocity is effective in increasing the maximum lift. An investigation was therefore conducted in the Langley high-speed 7- by 10-foot tunnel over a Mach number range from about 0.10 to 0.80 and over a pitching-velocity range from nearly 0 to about 20 radians per second. Because of improvements in instrumentation the results presented herein supersede those given in reference 1.

SYMBOLS

b	span, feet
BM	wing bending moment, foot-pounds about 16.5-percent-semispan location
$\bar{c}$	mean aerodynamic chord, feet
C_L	lift coefficient $\left(\frac{L}{qS}\right)$
$C_{L_{max}}$	maximum lift coefficient
C_{BM}	bending-moment coefficient $(4BM/qSb)$
L	lift, pounds
M	Mach number
n	acceleration normal to relative wind, feet per second per second
q	dynamic pressure, pounds per square foot
R	Reynolds number
V	true airspeed, feet per second
S	wing area, square feet
α	angle of attack, degrees

$d\alpha/dt$ rate of change of angle of attack (pitching velocity), radians per second

$\frac{\bar{c}}{V}\frac{d\alpha}{dt}$ dimensionless pitching-velocity parameter, change in angle of pitch per chord traveled, radians

APPARATUS

The apparatus and model were essentially as described in reference 1. A diagrammatic sketch of the pitching-model apparatus and a photograph of the model mounted in the Langley high-speed 7- by 10-foot tunnel are presented in figures 1 and 2, respectively. Briefly, the model was a $\frac{1}{20}$-scale partial reproduction of a conventional single-engine fighter airplane with an elliptical wing of modified NACA 230-series sections. The 2-foot-span wing and truncated propellerless fuselage of the model was designed to rotate in pitch with approximately constant rates from a small negative angle through the angle of maximum lift. The design permitted a short pause at the negative angle to permit resumption of steady-flow conditions prior to each pull-up. Modifications were made to the original apparatus to change the starting angle of pitch from about $-6\frac{1}{2}^\circ$ to $-3\frac{1}{2}^\circ$ and to install wing-bending-moment gages on the left wing at the $16\frac{1}{2}$-percent-semispan location. The wing had not been designed for wing-bending-moment measurements and the low stress level did not permit a stable drift-free installation but was suitable for qualitative measurements. Because the flexure type of lift measuring device used (see fig. 1) was inherently subject to the acceleration forces of the model in the lift direction, an accelerometer was installed to permit corrections for this effect, which was expected to be larger in the present tests because of the increased pitching-velocity range.

METHOD AND RESULTS

Time variations of lift, wing bending moment, angle of attack, and acceleration were recorded during pull-ups for pitching velocities varying from nearly 0 to about 20 radians per second. The investigation covered the Mach number range from 0.10 to 0.80 with incremental steps of about 0.05 Mach number. The variation of tunnel Reynolds number with Mach number during the tests is given in figure 3. Owing to limitations of the available torque of the pitching mechanism the maximum angle of attack attained during the pull-ups diminished with increasing Mach number

from a maximum value of 30° at Mach numbers below about 0.30 to a value of about 15° at a Mach number of 0.80.

Figure 4 shows scale reproductions of test records obtained during the investigation which give typical time variations of the aforementioned variables for various Mach numbers and pitching velocities. Treatment of the data was similar to that in reference 1 except for the inclusion of acceleration corrections for the present test data. Corrections for the inertia forces occurring during the pull-up were applied when necessary by the approximate method of diminishing the peak values of the lift trace an amount proportional to the mean value of the acceleration during the time of peak lift (fig. 4(b)). For Mach numbers above 0.60, the lift and bending moment increased continuously up to the highest angles attained by the model (fig. 4(c)) so that in contrast to that at the lower Mach numbers no definite aerodynamic maximums were obtained. In figure 4(c), the acceleration is given only by an approximate envelope defined by two dash lines because of the difficulty of reproduction of the multifrequency oscillations produced at high speeds by tunnel vibration and flow fluctuations.

The lift-coefficient characteristics of the model as cross-plotted from records for nearly zero pitching velocity are presented in figure 5. The curves were checked at several points by measuring the lift at various fixed angles of attack.

In figure 6, the maximum pitching-velocity effect on the characteristics of C_L is compared with that on the characteristics of C_{BM} for various Mach numbers in the 0.20 to 0.60 range wherein angle of attack is the independent variable. The solid curves give the variations for the steady condition (approx. zero pitching velocity); whereas the dash parts show the maximum extension of the curves due to the effect of pitching velocity.

The maximum values of the lift coefficient obtained for each test value of the pitching velocity are given by the round test points in figure 7 for all test Mach numbers up to 0.60. Each test point represents an average of the readings obtained from a group of pull-ups all at a nearly constant value of $d\alpha/dt$. The applicable $d\alpha/dt$ was taken as the slope of the line joining the point on the angle-of-attack – time record corresponding to zero lift with the point corresponding to peak lift. (See reference 1.) The square test points at $M = 0.55$ and 0.60 are values of the lift coefficient corresponding to points on the original records at which pronounced changes occurred in the slopes of lift and bending moment against time.

In figure 8, $C_{L_{max}}$ is shown as a function of the change in angle of pitch per chord traveled $\left(\frac{\bar{c}}{V}\frac{d\alpha}{dt}\right)$ for various Mach numbers. The

dash lines representing Mach numbers above 0.60 were drawn at values of the lift coefficient corresponding to the maximum angles attained at each Mach number.

The variation of maximum lift coefficient with Mach number for various values of $\frac{\bar{c}}{V}\frac{d\alpha}{dt}$ is presented in figure 9. The envelope curve labeled "Limit $C_{L_{max}}$" is not given for a constant value of $\frac{\bar{c}}{V}\frac{d\alpha}{dt}$ as are the other curves but represents the highest value of $C_{L_{max}}$ obtained at each Mach number. The upper dash curve gives the lift coefficients at the maximum angles attained. The lower dash curve labeled "C_L at initial separation" represents values of the lift coefficient corresponding to points of inflection on the original records similar to those described previously in connection with figure 7 for Mach numbers of 0.55 and 0.60. These points on the original records were also identifiable (but less definitely so) by the noticeable increase in trace vibration as the angle of attack was further increased.

DISCUSSION

The variation of the maximum lift coefficient with pitching velocity is best illustrated in figures 7 and 8. For the Mach number range below about 0.55, $C_{L_{max}}$ increases in a generally linear manner with pitching velocity to a maximum value which appears relatively independent of further increases in pitching velocity. At the lowest Mach numbers moderate deviations from linearity are evident. The leveling off occurs at progressively smaller values of $\frac{\bar{c}}{V}\frac{d\alpha}{dt}$ as the Mach number is increased. In figure 7, the scatter of the data is moderate for pitching velocities up to and slightly beyond the knees of the curves. For this range of pitching velocity the inertia forces were found to be negligible and the accuracy of the results approaches the instrument accuracy for static conditions which in general is within about 2 percent. For higher pitching velocities the inertia forces were no longer negligible and the greater scatter in this region is a measure of the somewhat limited accuracy with which acceleration corrections could be made. Since for these higher pitching velocities the variation of the data followed no definite pattern with Mach number the curves of $C_{L_{max}}$ were extended level at a value equal to that at the knees.

The magnitude of the pitching-velocity effect on $C_{L_{max}}$ (fig. 9) is seen to be largest at the lower Mach numbers where nearly a two-fold increase occurs. The total increment in $C_{L_{max}}$ due to pitching velocity decreases with increasing Mach number and in the 0.55 to 0.60 Mach number region the curve of limit $C_{L_{max}}$ merges with the curve for zero pitching velocity. If the mean slopes of the curves of $C_{L_{max}}$ plotted against pitching velocity in figure 8 are considered a measure of the influence of pitching velocity on the lift, then the fact that these slopes increase generally with Mach number suggests that the decreasing total increment of $C_{L_{max}}$ may be caused by some limiting local flow condition on the wing. The similarity in shape of the curves below a Mach number of 0.40 in figure 9 also suggests that the interrelated effects of Mach and Reynolds numbers on maximum lift in this region are similar with or without pitching velocity.

The curve labeled "C_L at initial separation" was included in figure 9 because it defines approximately the lift-coefficient boundary at which the condition typified by pre-maximum-lift flow separation occurs. This fact is evident both from the manner in which the data were obtained (see section entitled "Method and Results") and the fact that the values along this curve occur near the knee or force break on the lift-coefficient curves of figure 5. Also, the curve corresponds roughly with the buffet boundary which has been observed from various flight tests of this type airplane. It is of interest to note that as M is increased the effects of $d\alpha/dt$ become negligible at those Mach numbers at which pre-maximum-lift flow separation first begins to occur. This condition is in agreement with results of flight tests of a number of airplanes.

An indication of the spanwise variation of the pitching-velocity effect can be obtained from a comparison of the lift and bending-moment-coefficient characteristics presented in figure 6. For the low Mach number range up to 0.40 both coefficients reach their maximums at approximately the same angle of attack with or without pitching velocity. Without pitching velocity the flatness of the curves of C_{BM} in the stalling region relative to the curves of C_L indicates a gradual outboard progression of stall; whereas with pitching velocity the comparable sharpness of the peaks indicates a simultaneous and rather sharp stall over the greater part of the span.

At Mach numbers higher than about 0.40, the initial or partial flow separation (which is evidenced by the early deviations from linearity in the curves) is delayed to higher angles of attack due to the effects of pitching velocity. This delay of the initial separation is first seen at a lower Mach number for the curves of C_{BM} (M = 0.45) than for the

curves of C_L ($M = 0.55$). At sufficiently high angles of attack, however, larger values of the coefficients can be obtained without the necessity of pitching velocity. The unsteady-force-break values of the lift coefficient as a function of pitching velocity for Mach numbers of 0.55 and 0.60 were presented as the square test points in figure 7 to illustrate this effect.

SUMMARY OF RESULTS

The effect of rate of change of angle of attack on the lift of a small model of a conventional fighter airplane over the Mach number range from 0.10 to 0.80 are summarized as follows:

For Mach numbers below about 0.55, the maximum lift coefficient increased linearly with pitching velocity to a maximum value which appeared relatively independent of further increases of pitching velocity. The total increment of the maximum lift coefficient with pitching velocity was largest (about 100 percent) at the lower Mach numbers; it decreased with increasing Mach number and became negligible for Mach numbers above about 0.55. In contrast, the rate of increase of the maximum lift coefficient with the pitching-velocity factor increased generally with Mach number. Both the limit value of the maximum lift coefficient and the value of the pitching-velocity factor at which it occurred decreased continuously with increasing Mach number.

Langley Aeronautical Laboratory
National Advisory Committee for Aeronautics
Langley Air Force Base, Va., January 10, 1950

REFERENCE

1. Harper, Paul W., and Flanigan, Roy E.: Investigation of the Variation of Maximum Lift for a Pitching Airplane Model and Comparison with Flight Results. NACA TN 1734, 1948.

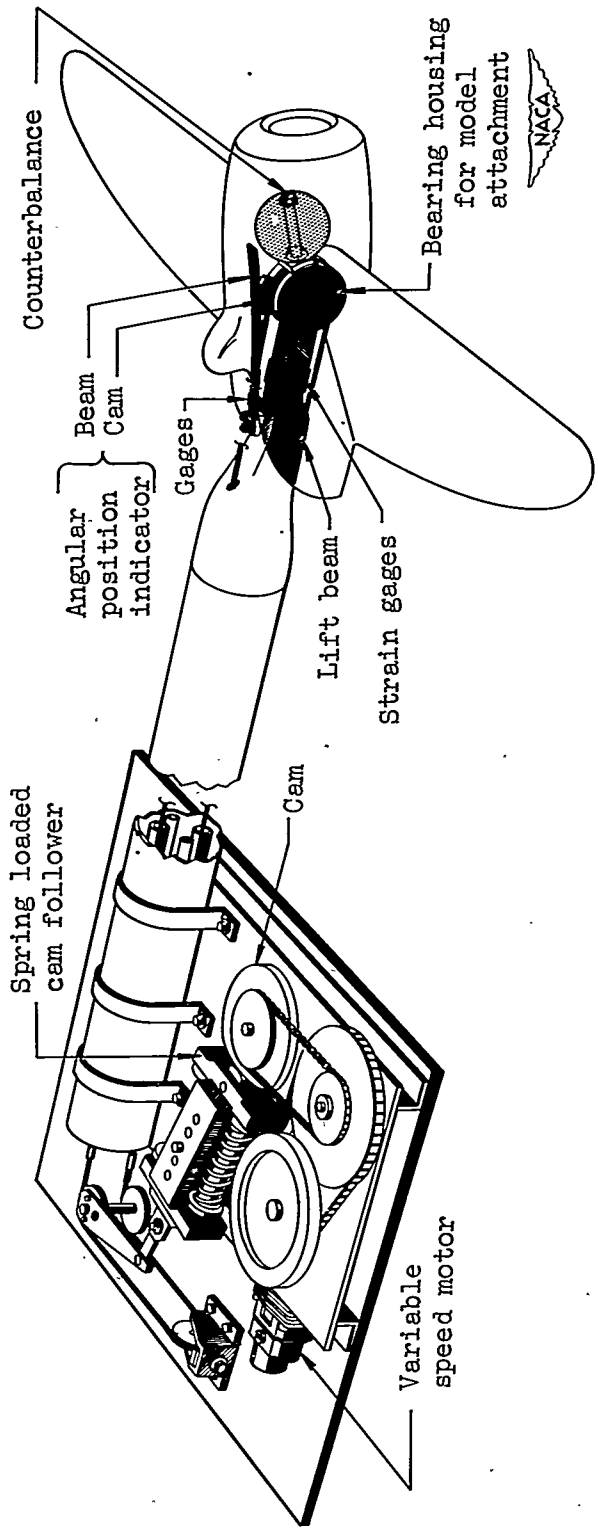

Figure 1.- Pitching-model apparatus.

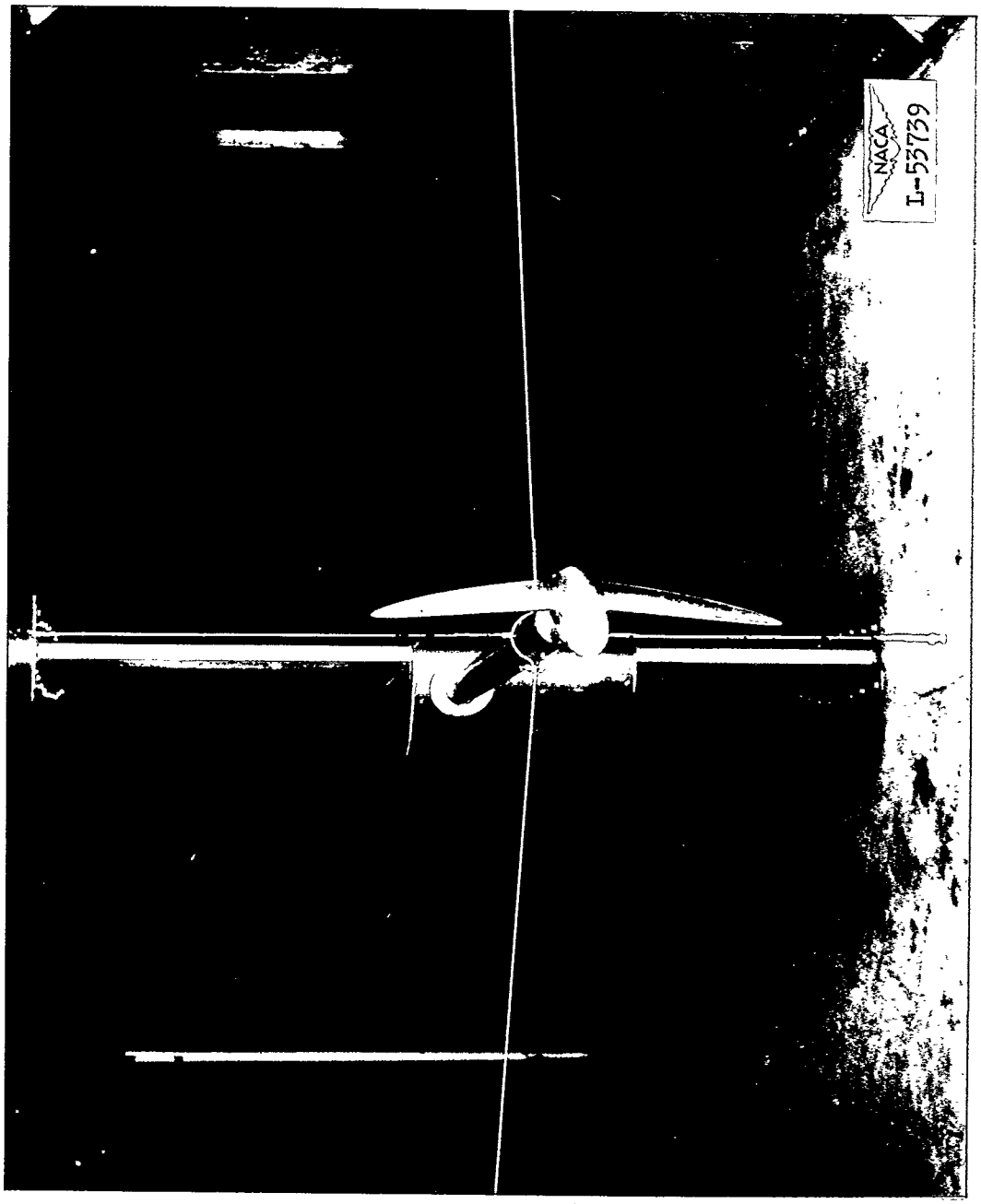

Figure 2.- The pitching model mounted in the Langley high-speed 7- by 10-foot tunnel.

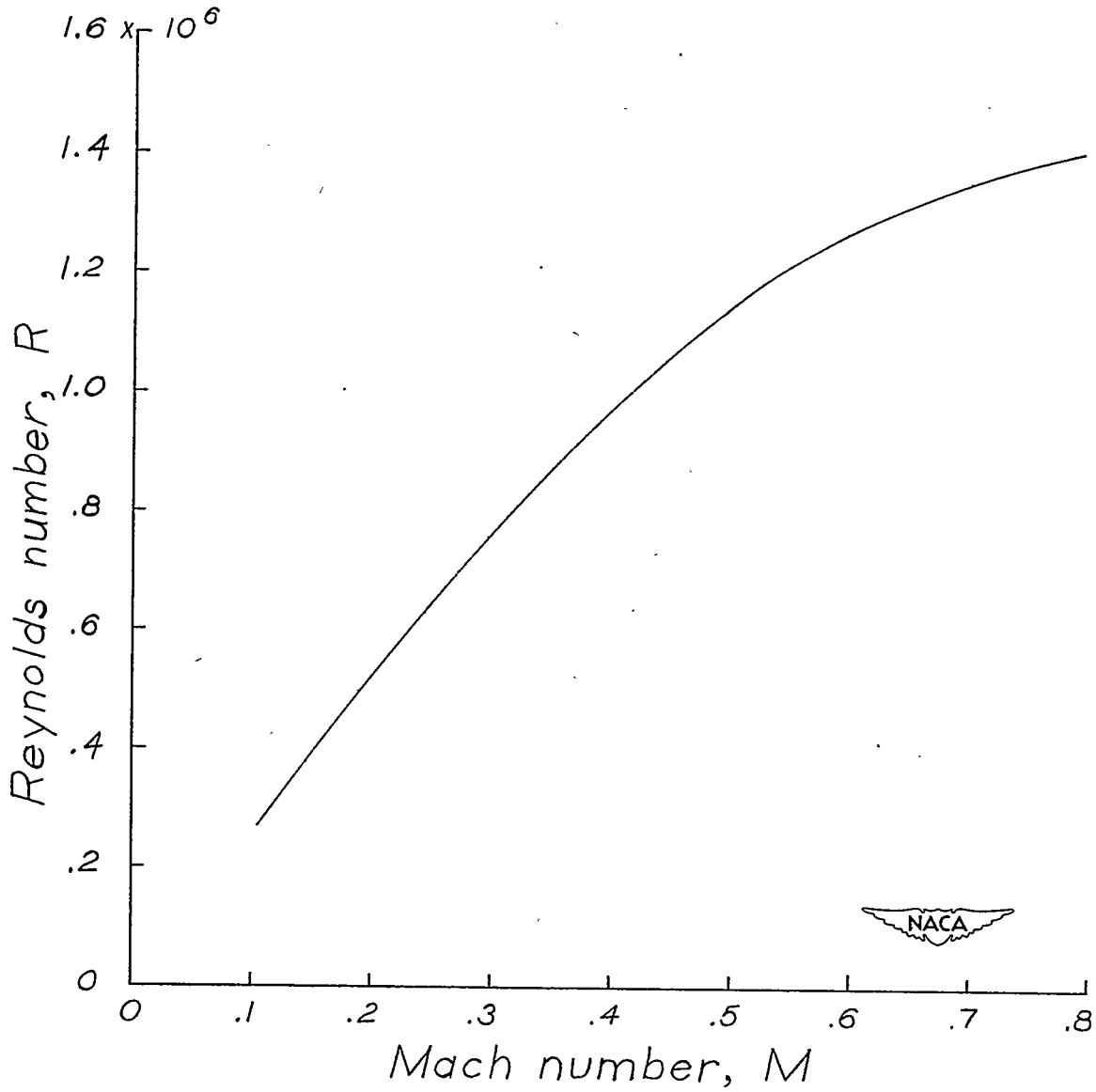

Figure 3.- Variation of Reynolds number with Mach number for the pitching-model tests.

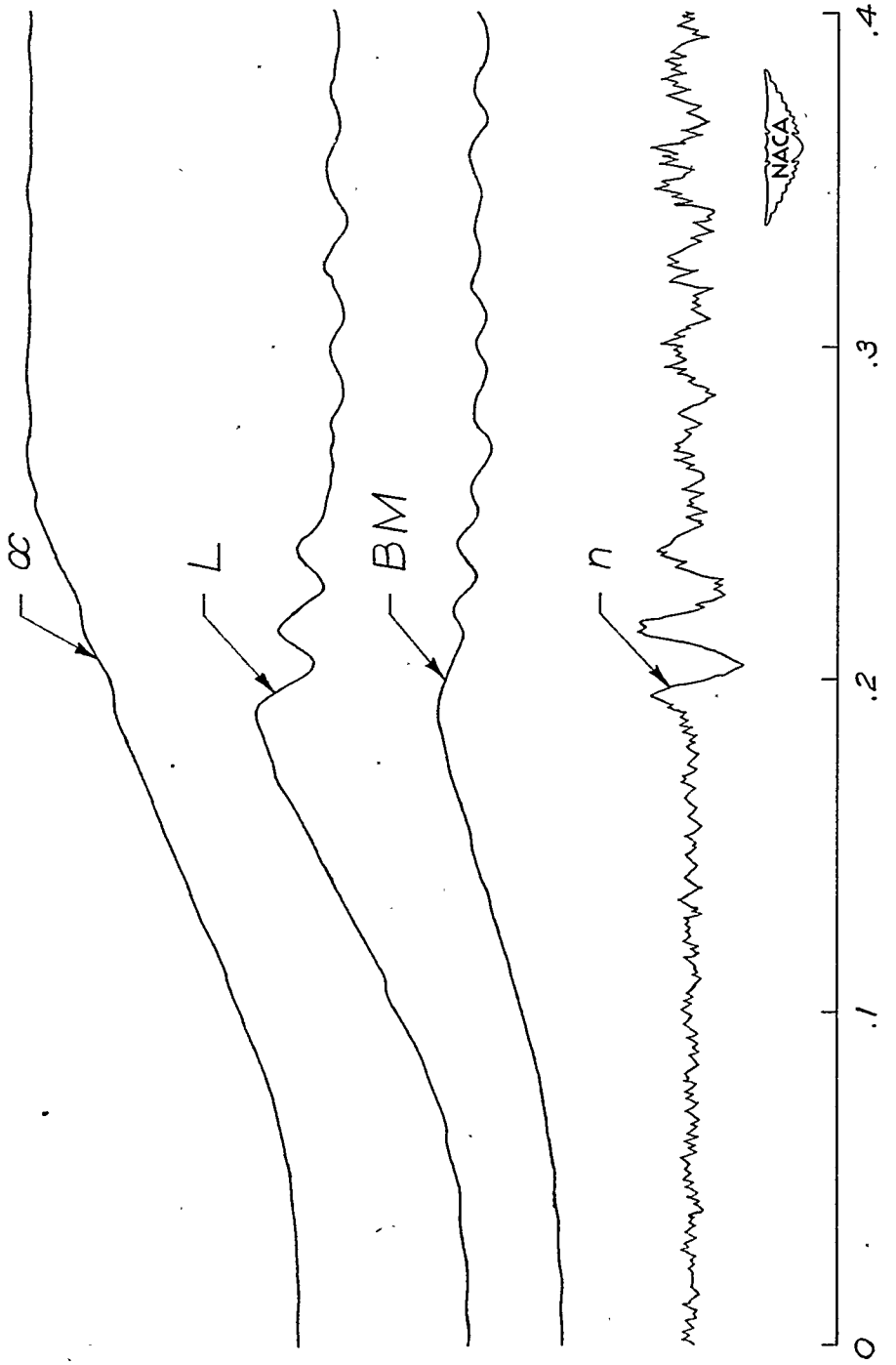

(a) M = 0.35; $\frac{d\alpha}{dt}$ = 2.7.

Figure 4.- Typical oscillograph records.

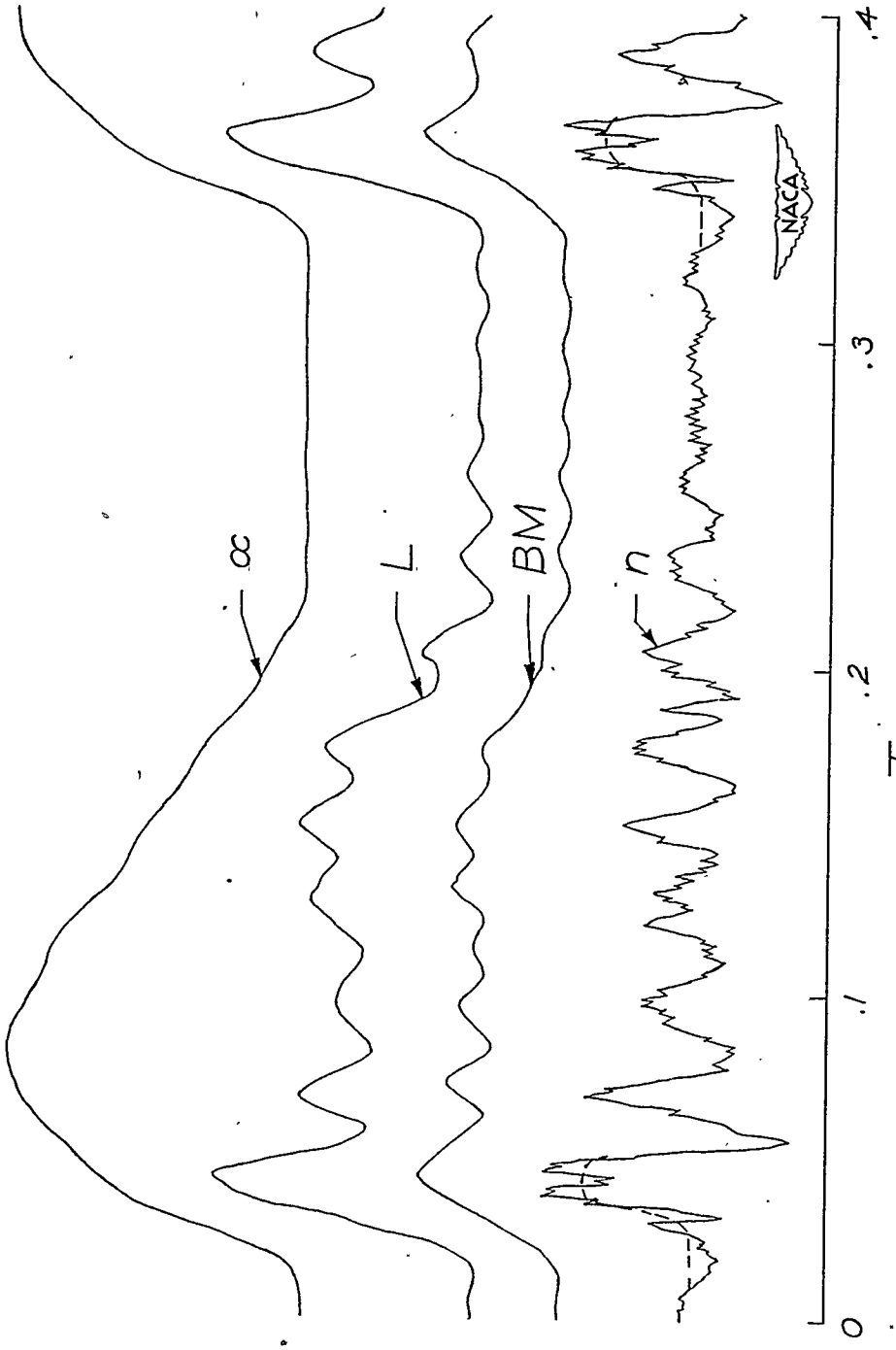

(b) M = 0.35; $\frac{d\alpha}{dt}$ = 14.4.

Figure 4.- Continued.

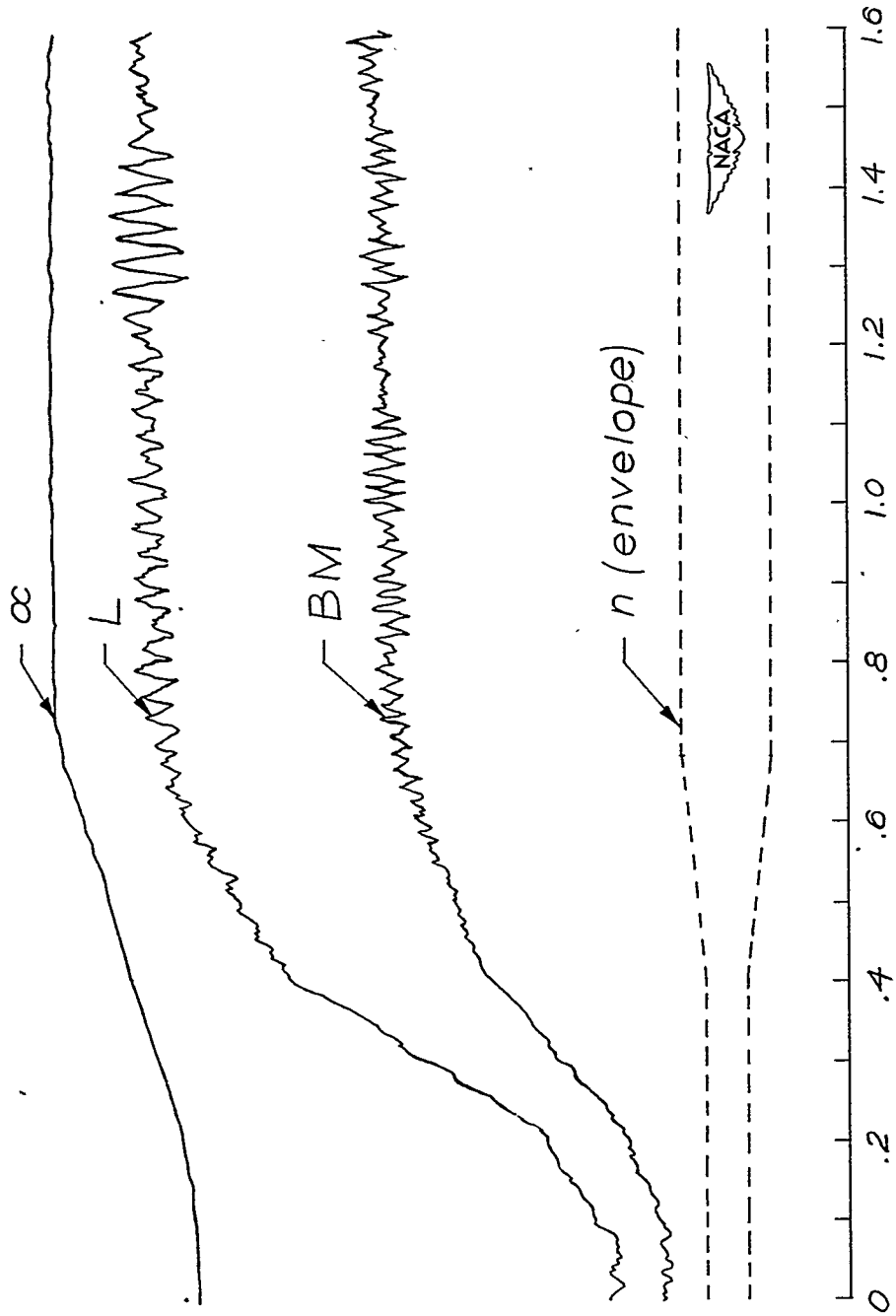

(c) M = 0.75; $\frac{d\alpha}{dt}$ = 0.5.

Figure 4.- Concluded.

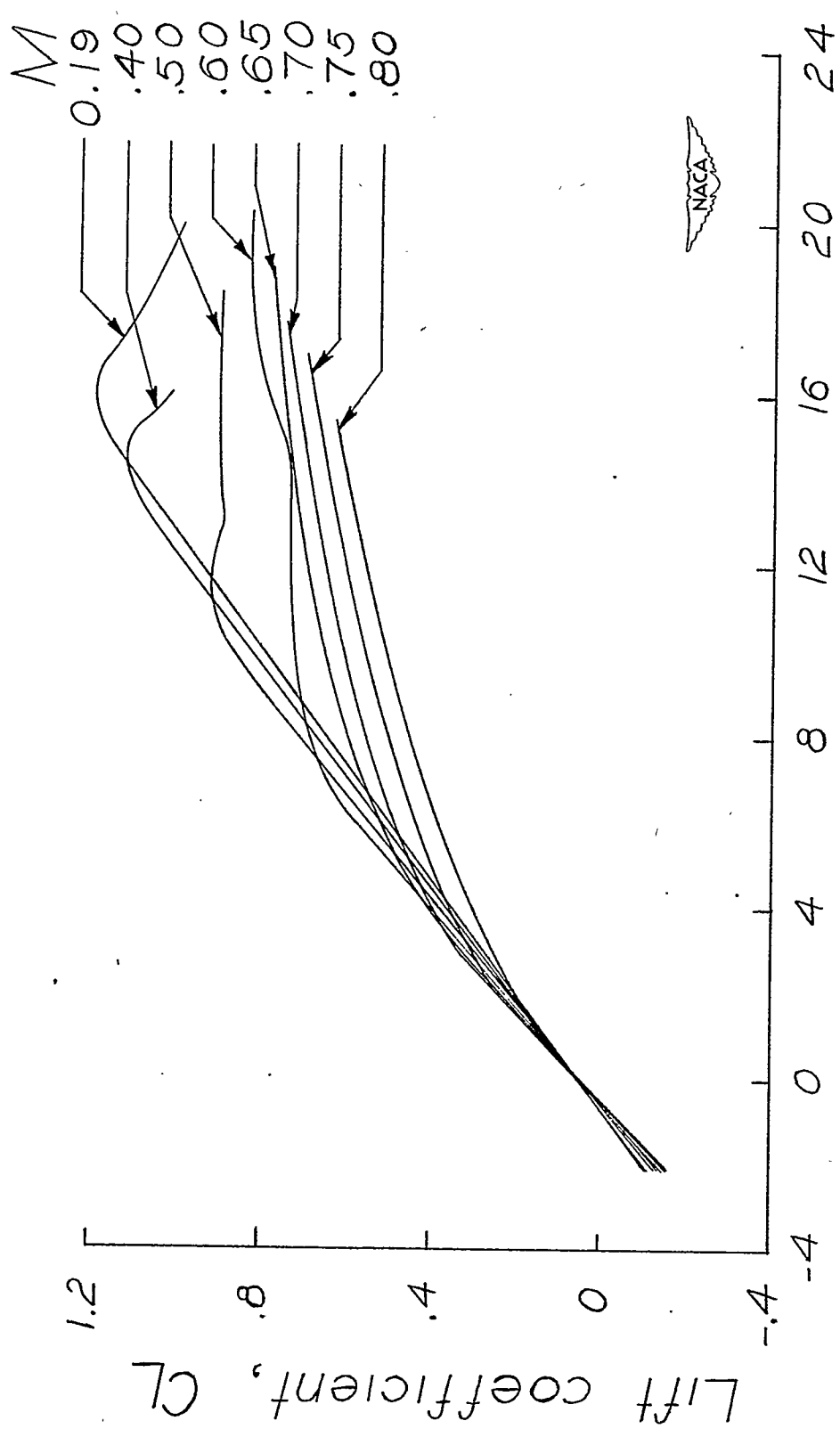

Figure 5.- Lift characteristics of model at various Mach numbers for approximately zero pitching velocities.

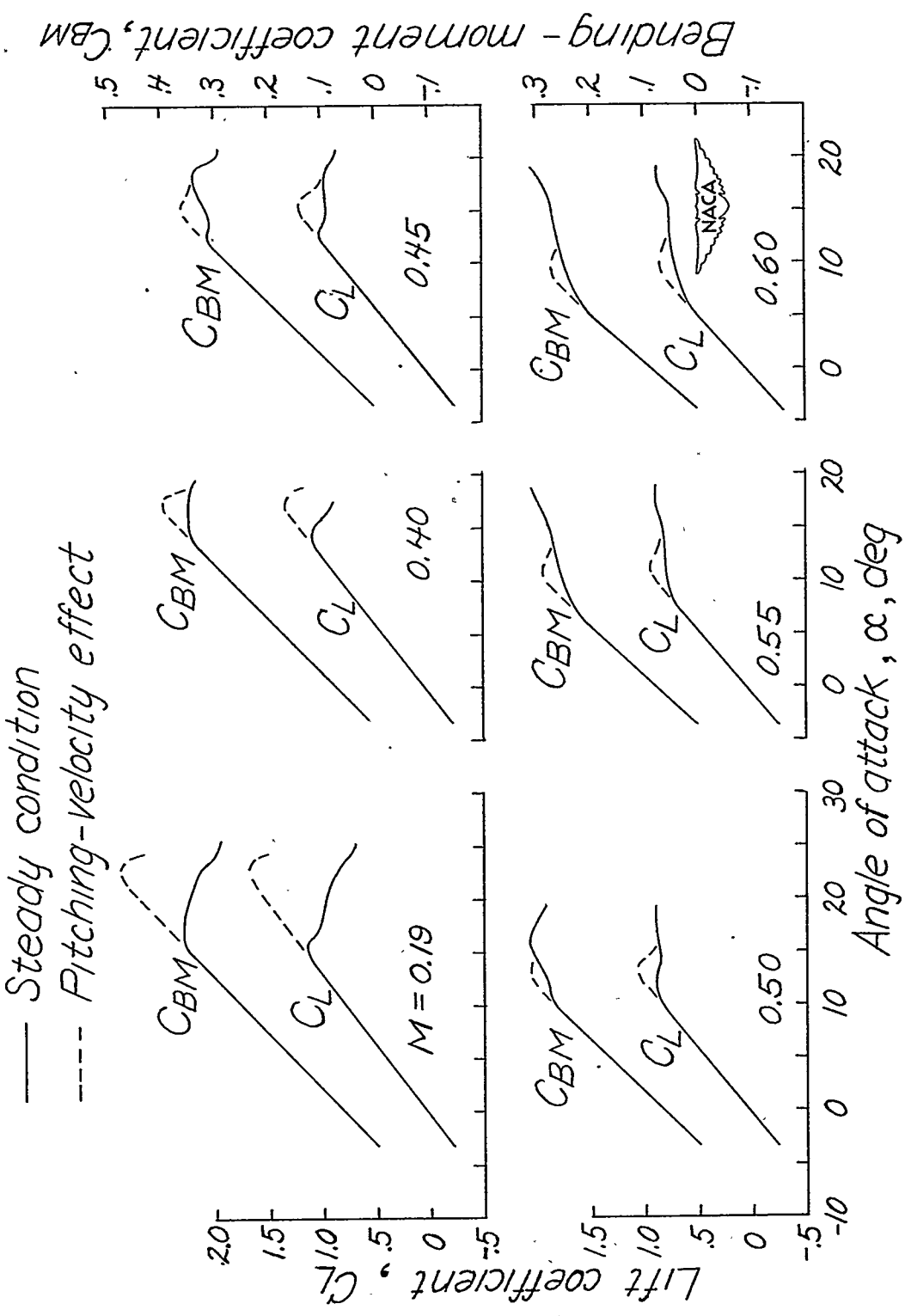

Figure 6.- Maximum pitching-velocity effect on lift and bending-moment characteristics for various Mach numbers.

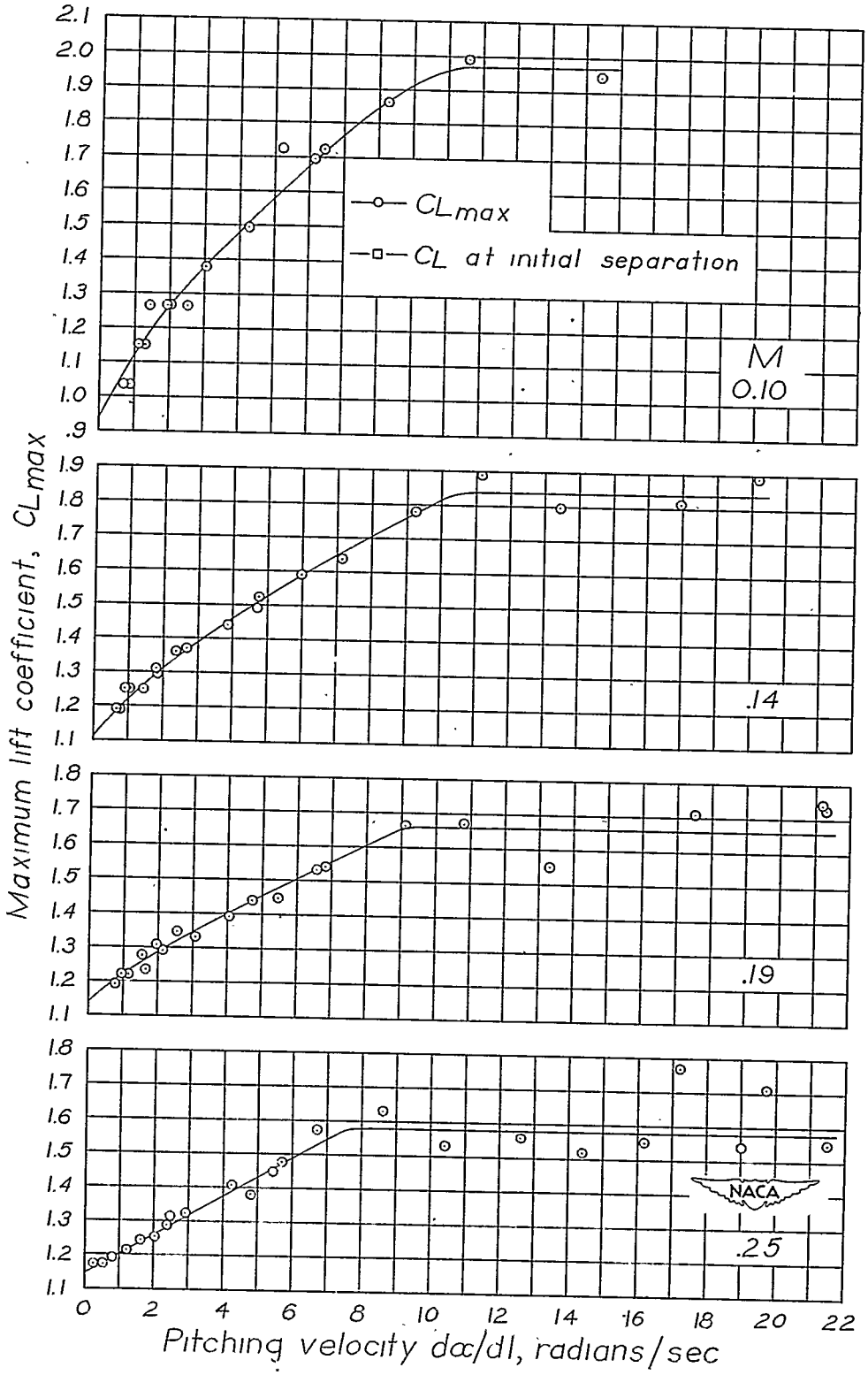

Figure 7.- Variation of maximum lift coefficient with pitching velocity.

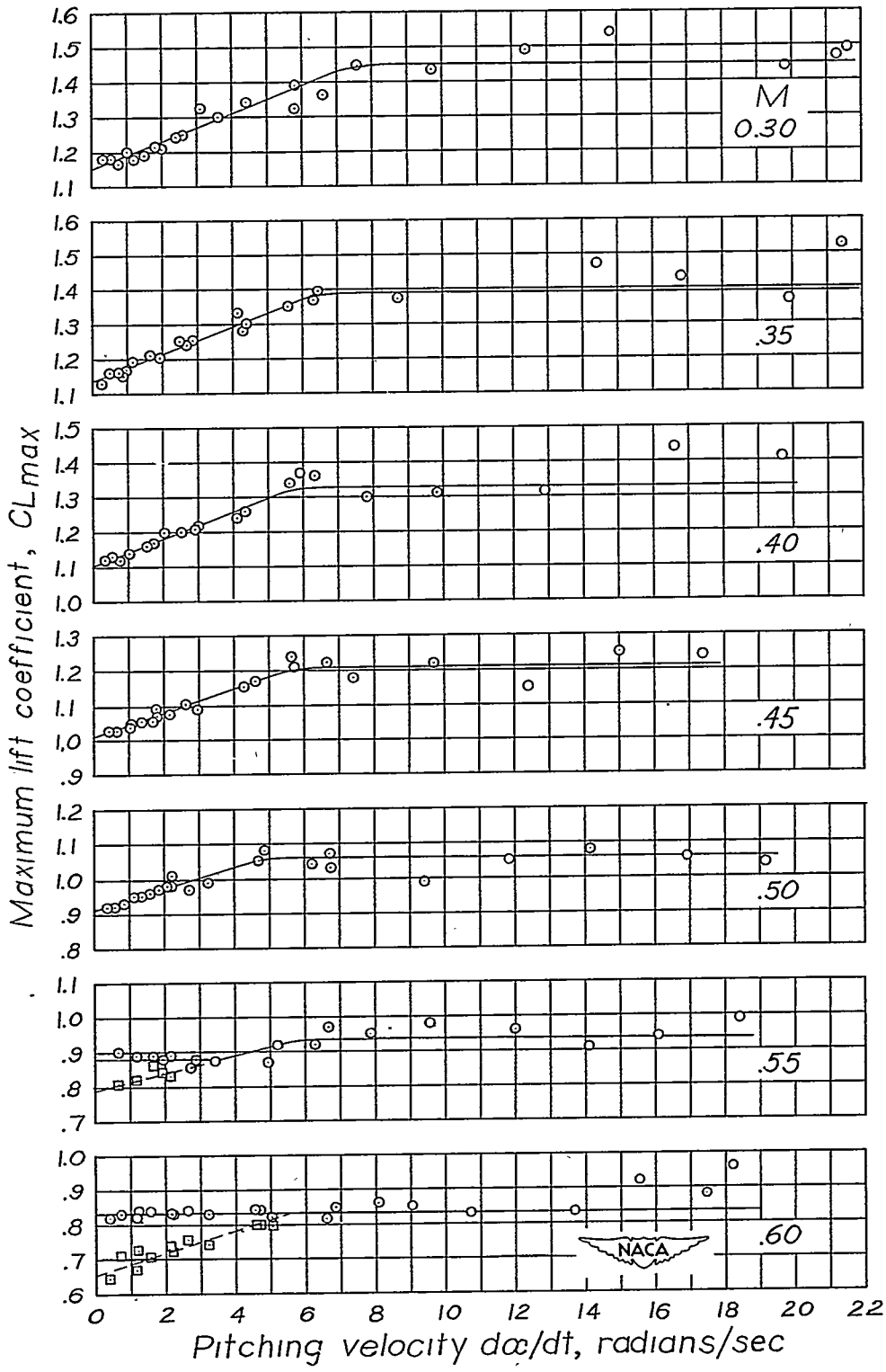

Figure 7.- Concluded.

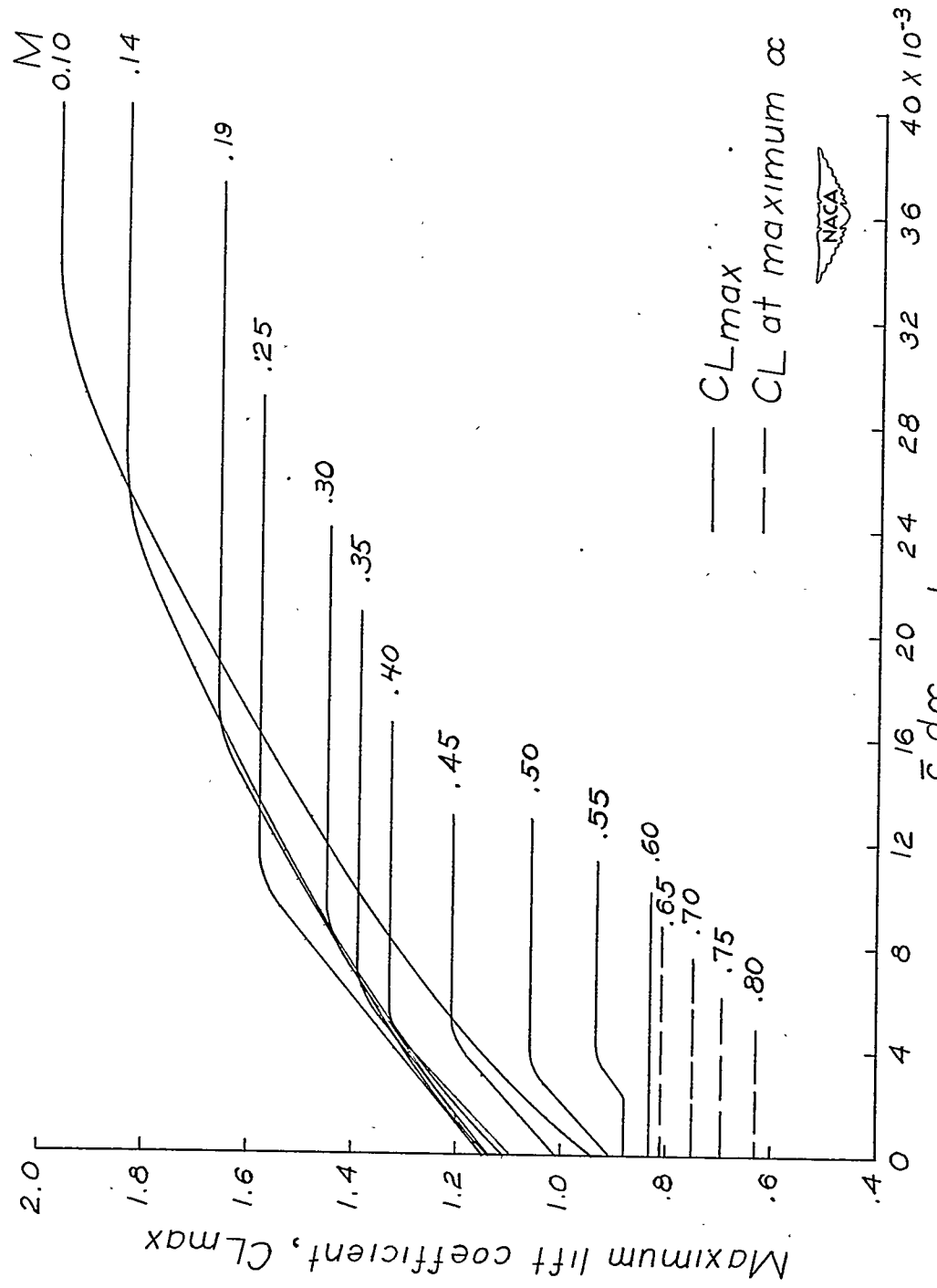

Figure 8.- Variation of maximum lift coefficient with change in angle of pitch per chord traveled.

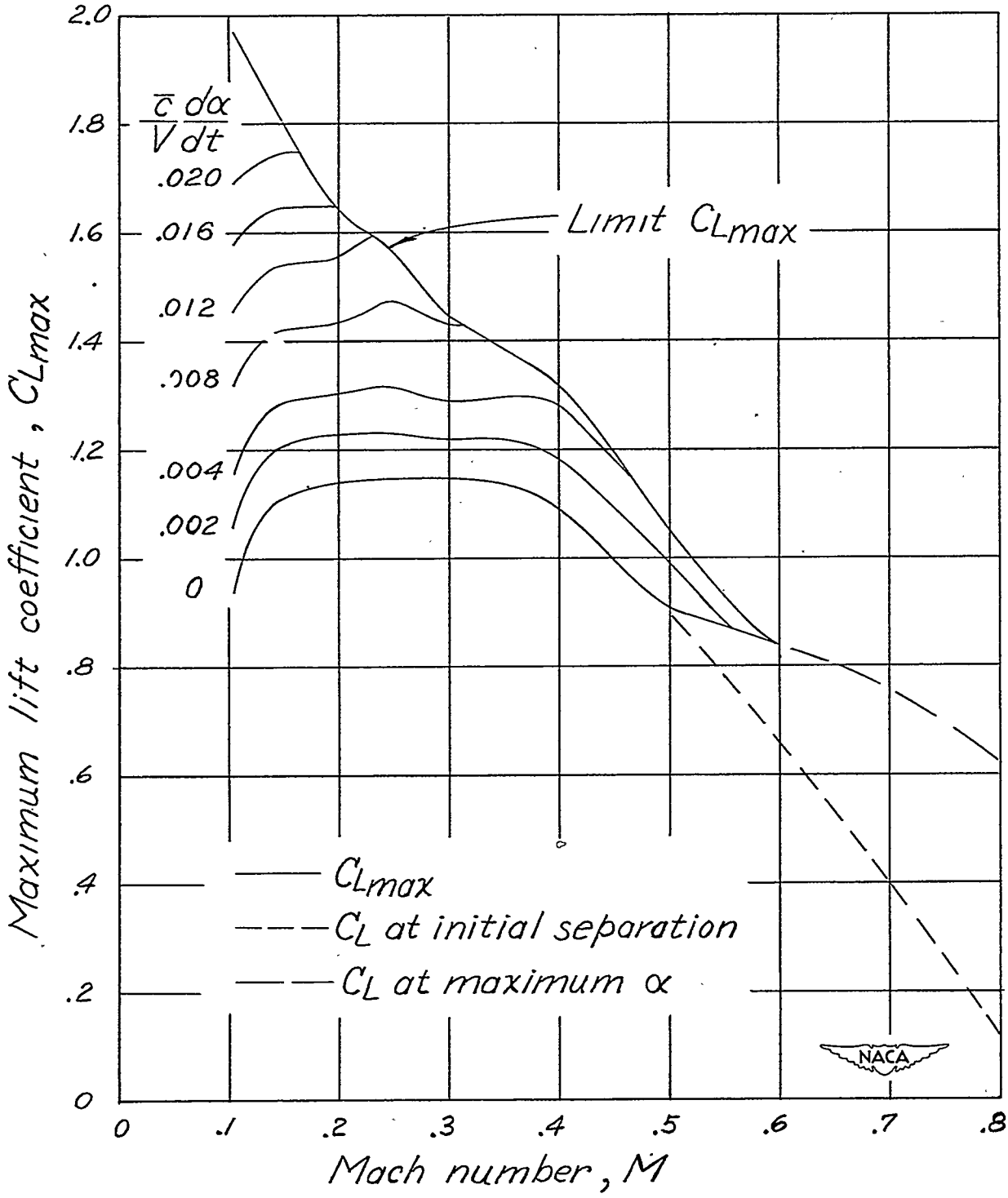

Figure 9.- The effect of Mach number on the maximum lift coefficient for various values of $\frac{\bar{c}}{V}\frac{d\alpha}{dt}$.

NACA-Langley - 3-23-50 - 1000